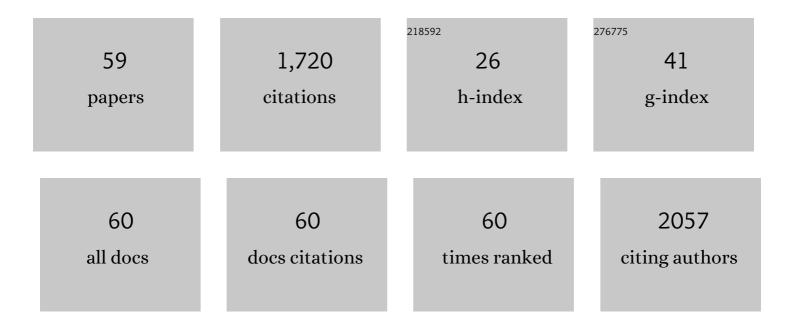
List of Publications by Year in descending order

Source: https://exaly.com/author-pdf/2416002/publications.pdf Version: 2024-02-01



MIHALA TANASE

#	Article	IF	CITATIONS
1	CNN-based burned area mapping using radar and optical data. Remote Sensing of Environment, 2021, 260, 112468.	4.6	46
2	Growing Stock Volume Retrieval from Single and Multi-Frequency Radar Backscatter. Forests, 2021, 12, 944.	0.9	4
3	Fire, drought and productivity as drivers of dead wood biomass in eucalypt forests of south-eastern Australia. Forest Ecology and Management, 2021, 482, 118859.	1.4	14
4	Shifts in Forest Species Composition and Abundance under Climate Change Scenarios in Southern Carpathian Romanian Temperate Forests. Forests, 2021, 12, 1434.	0.9	15
5	Investigating the Impact of Digital Elevation Models on Sentinel-1 Backscatter and Coherence Observations. Remote Sensing, 2020, 12, 3016.	1.8	11
6	Burned Area Detection and Mapping: Intercomparison of Sentinel-1 and Sentinel-2 Based Algorithms over Tropical Africa. Remote Sensing, 2020, 12, 334.	1.8	35
7	Structural diversity underpins carbon storage in Australian temperate forests. Global Ecology and Biogeography, 2020, 29, 789-802.	2.7	45
8	Retrieval of Forest Structural Parameters From Terrestrial Laser Scanning: A Romanian Case Study. Forests, 2020, 11, 392.	0.9	6
9	High-severity wildfires in temperate Australian forests have increased in extent and aggregation in recent decades. PLoS ONE, 2020, 15, e0242484.	1.1	32
10	Optimum Sentinel-1 Pixel Spacing for Burned Area Mapping. , 2020, , .		0
11	Are High Severity Fires Increasing in Southern Australia?. , 2020, , .		1
12	Deep Neural Networks for Forest Growing Stock Volume Retrieval: A Comparative Analysis for L-band SAR data. , 2020, , .		3
13	Title is missing!. , 2020, 15, e0242484.		0
14	Title is missing!. , 2020, 15, e0242484.		0
15	Title is missing!. , 2020, 15, e0242484.		0
16	Title is missing!. , 2020, 15, e0242484.		0
17	Estimating forest stand structure attributes from terrestrial laser scans. Science of the Total Environment, 2019, 691, 205-215.	3.9	12
18	Synthetic aperture radar sensitivity to forest changes: A simulations-based study for the Romanian forests. Science of the Total Environment, 2019, 689, 1104-1114.	3.9	28

#	Article	IF	CITATIONS
19	Burned area detection and mapping using Sentinel-1 backscatter coefficient and thermal anomalies. Remote Sensing of Environment, 2019, 233, 111345.	4.6	87
20	Estimating prescribed fire impacts and post-fire tree survival in eucalyptus forests of Western Australia with L-band SAR data. Remote Sensing of Environment, 2019, 224, 133-144.	4.6	21
21	Temporal Decorrelation of C-Band Backscatter Coefficient in Mediterranean Burned Areas. Remote Sensing, 2019, 11, 2661.	1.8	8
22	Remote sensing of βâ€diversity: Evidence from plant communities in a semiâ€natural system. Applied Vegetation Science, 2019, 22, 13-26.	0.9	23
23	Methods for tree cover extraction from high resolution orthophotos and airborne LiDAR scanning in Spanish dehesas. Revista De Teledeteccion, 2019, , 17.	0.6	6
24	Remote sensing for the Spanish forests in the 21st century: a review of advances, needs, and opportunities. Forest Systems, 2019, 28, eR001.	0.1	34
25	Evaluation of backscatter coefficient temporal indices for burned area mapping. , 2019, , .		0
26	Fire-severity classification across temperate Australian forests: random forests versus spectral index thresholding. , 2019, , .		6
27	Evaluation of Spectral Indices for Assessing Fire Severity in Australian Temperate Forests. Remote Sensing, 2018, 10, 1680.	1.8	64
28	The Polarimetric L-Band Imaging Synthetic Aperture Radar (PLIS): Description, Calibration, and Cross-Validation. IEEE Journal of Selected Topics in Applied Earth Observations and Remote Sensing, 2018, 11, 4513-4525.	2.3	15
29	Detection of windthrows and insect outbreaks by L-band SAR: A case study in the Bavarian Forest National Park. Remote Sensing of Environment, 2018, 209, 700-711.	4.6	52
30	L-band SAR sensitivity to prescribed burning effects in eucalypt forests of Western Australia. , 2018, , .		2
31	Insights into burned areas detection from Sentinel-1 data and locally adaptive algorithms. , 2018, , .		2
32	Temporal backscattering coefficient decorrelation in burned areas. , 2018, , .		0
33	An Extension of the Alpha Approximation Method for Soil Moisture Estimation Using Time-Series SAR Data Over Bare Soil Surfaces. IEEE Geoscience and Remote Sensing Letters, 2017, 14, 1328-1332.	1.4	20
34	Soil Moisture Retrieval in Agricultural Fields Using Adaptive Model-Based Polarimetric Decomposition of SAR Data. IEEE Transactions on Geoscience and Remote Sensing, 2016, 54, 4445-4460.	2.7	35
35	Mortality and recruitment of fire-tolerant eucalypts as influenced by wildfire severity and recent prescribed fire. Forest Ecology and Management, 2016, 380, 107-117.	1.4	86
36	Monitoring live fuel moisture in semiarid environments using L-band radar data. International Journal of Wildland Fire, 2015, 24, 560.	1.0	19

#	Article	IF	CITATIONS
37	Fire severity estimation from space: a comparison of active and passive sensors and their synergy for different forest types. International Journal of Wildland Fire, 2015, 24, 1062.	1.0	37
38	Detecting and Quantifying Forest Change: The Potential of Existing C- and X-Band Radar Datasets. PLoS ONE, 2015, 10, e0131079.	1.1	20
39	Validation of Canopy Height Profile methodology for small-footprint full-waveform airborne LiDAR data in a discontinuous canopy environment. ISPRS Journal of Photogrammetry and Remote Sensing, 2015, 104, 144-157.	4.9	39
40	Radar Burn Ratio for fire severity estimation at canopy level: An example for temperate forests. Remote Sensing of Environment, 2015, 170, 14-31.	4.6	52
41	Forest Fire Severity Assessment Using ALS Data in a Mediterranean Environment. Remote Sensing, 2014, 6, 4240-4265.	1.8	46
42	Polarimetric Properties of Burned Forest Areas at C- and L-Band. IEEE Journal of Selected Topics in Applied Earth Observations and Remote Sensing, 2014, 7, 267-276.	2.3	39
43	Effective LAI and CHP of a Single Tree From Small-Footprint Full-Waveform LiDAR. IEEE Geoscience and Remote Sensing Letters, 2014, 11, 1634-1638.	1.4	13
44	Estimation of soil surface roughness of agricultural soils using airborne LiDAR. Remote Sensing of Environment, 2014, 140, 107-117.	4.6	39
45	Evaluation of IEM, Dubois, and Oh Radar Backscatter Models Using Airborne L-Band SAR. IEEE Transactions on Geoscience and Remote Sensing, 2014, 52, 4966-4979.	2.7	62
46	Sensitivity of L-Band Radar Backscatter to Forest Biomass in Semiarid Environments: A Comparative Analysis of Parametric and Nonparametric Models. IEEE Transactions on Geoscience and Remote Sensing, 2014, 52, 4671-4685.	2.7	22
47	Forest Biomass Estimation at High Spatial Resolution: Radar Versus Lidar Sensors. IEEE Geoscience and Remote Sensing Letters, 2014, 11, 711-715.	1.4	15
48	Airborne multi-temporal L-band polarimetric SAR data for biomass estimation in semi-arid forests. Remote Sensing of Environment, 2014, 145, 93-104.	4.6	52
49	The Soil Moisture Active Passive Experiments (SMAPEx): Toward Soil Moisture Retrieval From the SMAP Mission. IEEE Transactions on Geoscience and Remote Sensing, 2014, 52, 490-507.	2.7	154
50	Estimation of forest biomass from L-band polarimetric decomposition components. , 2013, , .		4
51	Preliminary leaf area index estimates from airborne small footprint full-waveform LiDAR data. , 2013, , .		3
52	Forest biomass estimation using radar and lidar synergies. , 2013, , .		3
53	Estimating burn severity at the regional level using optically based indices. Canadian Journal of Forest Research, 2011, 41, 863-872.	0.8	42
54	Soil moisture limitations on monitoring boreal forest regrowth using spaceborne L-band SAR data. Remote Sensing of Environment, 2011, 115, 227-232.	4.6	76

#	Article	IF	CITATIONS
55	Sensitivity of SAR data to post-fire forest regrowth in Mediterranean and boreal forests. Remote Sensing of Environment, 2011, 115, 2075-2085.	4.6	77
56	TerraSAR-X Data for Burn Severity Evaluation in Mediterranean Forests on Sloped Terrain. IEEE Transactions on Geoscience and Remote Sensing, 2010, 48, 917-929.	2.7	30
57	Sensitivity of X-, C-, and L-Band SAR Backscatter to Burn Severity in Mediterranean Pine Forests. IEEE Transactions on Geoscience and Remote Sensing, 2010, 48, 3663-3675.	2.7	86
58	Properties of X-, C- and L-band repeat-pass interferometric SAR coherence in Mediterranean pine forests affected by fires. Remote Sensing of Environment, 2010, 114, 2182-2194.	4.6	62
59	An Examination of the Effects of Spatial Resolution and Image Analysis Technique on Indirect Fuel Mapping. IEEE Journal of Selected Topics in Applied Earth Observations and Remote Sensing, 2008, 1, 220-229.	2.3	15